World Journal of Pharmaceutical Science and Research

www.wjpsronline.com

Research Article

ISSN: 2583-6579
SJIF Impact Factor: 6.916
Year - 2026
Volume: 5; Issue: 8
Page: 334-354

FABRICATION AND *IN-VITRO* CHARACTERIZATION OF RESVERATROL ENCAPSULATED POROUS BIOMIMETIC SKIN GRAFT FOR BURN TREATMENT

Vikash Kumar, Rajeev Ranjan, Dharmendra Kumar*

Narayan Institute of Pharmacy, Gopal Narayan Singh University, Jamuhar, Sasaram, Bihar- 821305.

Article Received: 02 June 2026 | | ***Article Revised: 23 June 2026*** | | ***Article Accepted: 14 July 2026***

***Corresponding Author: Dharmendra Kumar**
Narayan Institute of Pharmacy, Gopal Narayan Singh University, Jamuhar, Sasaram, Bihar- 821305.
DOI: https://doi.org/10.5281/zenodo.21705074

How to cite this Article: Vikash Kumar, Rajeev Ranjan, Dharmendra Kumar (2026) FABRICATION AND IN-VITRO CHARACTERIZATION OF RESVERATROL ENCAPSULATED POROUS BIOMIMETIC SKIN GRAFT FOR BURN TREATMENT. World Journal of Pharmaceutical Science and Research, 5(8), 334-354.

ABSTRACT

Introduction: Repair of deep third-degree burn wounds depends largely on effective skin cell proliferation and regeneration. In the present study, an antioxidant-incorporated biomimetic composite graft was developed and evaluated as a novel biomaterial for burn wound management. The fabrication of a resveratrol-encapsulated porous biomimetic skin graft offers a novel therapeutic strategy for effective burn wound management. Severe burns often involve excessive inflammation, oxidative stress, and delayed tissue regeneration, which can compromise healing outcomes. **Methods:** The resveratrol-loaded composite graft (gel–drug–PMS) was optimized at different resveratrol concentrations (2.5, 5, and 10 mg/mL) and characterized for physicochemical, and *in vitro* performance. Morphological evaluation was carried out using scanning electron microscopy, while cytomodulin coupling efficiency was quantified using the NanoOrange® assay. Thermal stability was assessed by micro-shrinkage temperature analysis using hot-stage microscopy. Antioxidant activity was evaluated by the DPPH free radical scavenging assay. Fluid uptake capacity was determined in phosphate-buffered saline (PBS), pH 7.4, and *in vitro* drug release, and degradation studies were performed. **Results:** The optimized formulation contained 10 mg/mL resveratrol, producing nanoparticles with a mean size of 602.5 nm (PDI 0.564). **Discussion:** The composite graft was stable at physiological temperature (37°C), retained significant antioxidant activity (SC_{50} = 6.8 µg/mL), absorbed approximately 50% of its weight in fluid, exhibited interconnected porous morphology, and achieved 83% cytomodulin coupling. **Conclusion:** These findings indicate that the developed biomimetic composite graft is a promising therapeutic approach for deep burn wound healing.

KEYWORDS: Biomimetic composite graft, Resveratrol, Deep burn wound, Antioxidant activity, Dermal regeneration.

INTRODUCTION

Severe thermal burns represent a major clinical challenge because they often result in extensive loss of skin tissue, which requires effective replacement strategies for proper healing and recovery.[1] One of the most promising approaches to address this problem is the use of tissue-engineered skin substitutes that can restore the structural and functional integrity of damaged skin.[2] Burn injuries continue to be a significant global health concern, causing substantial morbidity, long-term disability, and mortality worldwide. Each year, millions of individuals suffer from burn injuries that require medical attention and hospitalization.[3] Among these cases, a considerable proportion involves severe burns, particularly third-degree burns, which frequently lead to life-threatening complications. It has been estimated that more than 300,000 people worldwide die annually due to severe burn injuries.[3] Recent statistics indicate that in 2024 alone, burn-related injuries accounted for approximately 5,053 deaths.[4] In the United States, nearly 1.4 million individuals experience burn injuries each year, and approximately 54,000 to 180,000 of these patients require hospitalization for specialized treatment and care.[5]

Effective management of severe burn injuries requires timely medical intervention to prevent complications such as excessive fluid loss, microbial infection, and delayed wound healing.[6] Early surgical removal of necrotic tissue followed by appropriate wound coverage remains one of the most critical steps in the treatment of extensive burns. For many years, split-thickness skin autografts have been considered the gold standard treatment for full-thickness burn wounds due to their ability to promote rapid wound closure and integration with surrounding tissues.[7] However, the use of autografts is often associated with several limitations, including the availability of limited donor skin sites, the need for repeated surgical procedures, donor site morbidity, and increased patient discomfort.[8] These challenges have prompted researchers to explore alternative therapeutic strategies and to accelerate the development of advanced skin substitute technologies.[9]

Skin substitutes have emerged as promising alternatives for the treatment of severe burn injuries and extensive skin loss.[10] Currently, skin replacement systems are broadly categorized into three major types: epidermal equivalents, dermal equivalents, and composite equivalents that combine both dermal and epidermal components.[11] These engineered constructs aim to replicate the biological structure and functional properties of natural skin, thereby supporting tissue regeneration and improving wound healing outcomes.

The development of tissue-engineered skin represents a significant advancement in regenerative medicine and burn wound management. Tissue engineering integrates concepts from engineering, material science, and life sciences to design and develop biological substitutes capable of restoring, maintaining, or improving the function of damaged tissues.[12] Various tissue-engineered skin replacements have been investigated and developed, including cultured autologous keratinocyte grafts, allogenic keratinocyte sheets, autologous and allogenic composite grafts, acellular biological matrices, and cellular scaffolds.[2,13-15] Additionally, several biomaterials and biological components such as fibrin sealants, collagen-based matrices, and hyaluronic acid (HA) have been incorporated into skin substitutes to enhance cellular attachment, proliferation, and tissue regeneration.[16-19] In recent years, a number of skin substitute products have received approval from the U.S. Food and Drug Administration (FDA) and are currently available for clinical use in the management of burn wounds.[20-22]

In the present study, an attempt was made to develop an improved tissue-engineered graft designed specifically for the treatment of third-degree burn injuries. The objective of this research was to formulate a biodegradable, cost-effective,

and rapidly healing skin substitute that could potentially overcome some of the limitations associated with currently available commercial products. The developed graft formulation, referred to as Gel-drug-PMS, consisted of cytomodulin-coupled porous microparticles uniformly dispersed within a resveratrol-loaded gelatin hydrogel matrix. The composite structure was further stabilized through crosslinking with glutaraldehyde to enhance its mechanical stability and structural integrity. Cytomodulin, a biomimetic peptide, was incorporated to promote cellular growth, proliferation, and tissue regeneration, while resveratrol was included because of its well-known antioxidant and anti-inflammatory properties that can contribute to improved burn wound healing.[23] Based on the experimental findings presented in this study, the developed composite graft demonstrates promising potential as an effective therapeutic scaffold for the treatment and regeneration of third-degree burn wounds.

MATERIAL AND METHODS

Materials and solvents used for the experiments were of analytical grade. Resveratrol (Sigma Aldrich, USA), Gelatin (Sigma Aldrich, USA), Ketamine hydrochloride Injection IP, Aneket® (Neon Laboratories Ltd., India), Xylazine Injection, Xylaxin® (Indian Immunologicals Ltd., India), Cytomodulin (USV Ltd., Mumbai, India), Tegaderm® (3 M, Germany), Micropore® (3 M, Germany) were procured for the experiments.

HPLC method development and revalidation for determination of resveratrol

Chromatographic separation and reagent preparation

HPLC analytical method was developed for *in vitro* quantitative determination of resveratrol. Chromatographic separation was done using the Inertsil ODS-3 C18 (5 µm, 250 mm x 4.6 mm) column [24]. Mobile phase consisted of acetonitrile: ammonium acetate buffer (pH 3.5, 45:55) in isocratic mode. Mobile phase solvents were filtered through 0.22 µm nylon filter and degassed in ultrasonic bath sonicator for 60 min before using them. A stock solution of the drug was prepared at the strength of 50µg/ml. It was diluted with phosphate buffer (10 mM; pH 3.5, 5% tween 80) to prepare dilutions ranging in concentrations from 2-20 µg/ml of the drug. The solutions were injected in triplicate into the HPLC column. Detection was carried out at 306 nm for resveratrol using PDA detector. Flow rate was kept at 1 ml/min. The developed method was then validated for linearity, accuracy, precision and specificity as per the ICH guidelines.

HPLC method revalidation

Linearity

The linearity of the analytical method was assessed by constructing a calibration curve between the detector response (peak area) and the corresponding analyte concentrations. Linear regression analysis was performed to determine the slope, intercept, and correlation coefficient (R^2) of the calibration curve, which reflects the degree of linear relationship between concentration and response.

Accuracy

The accuracy of the method was evaluated by measuring the amount of resveratrol present in quality control (QC) samples with known concentrations that differed from those used for the calibration curve. The results were expressed in terms of percentage recovery. For this assessment, three QC concentration levels were analyzed in triplicate, and the procedure was repeated three times per day over three consecutive days.

Precision

The precision of the analytical procedure was expressed as the relative standard deviation (RSD) and was determined by evaluating both intra-day and inter-day variations. Intra-day precision was determined by analyzing three different concentrations of the drug in triplicate within the same day. Inter-day precision was assessed by performing the same analysis on three consecutive days using identical experimental conditions.

Specificity

Specificity refers to the ability of the analytical method to accurately measure the drug in the presence of formulation components such as gelatin. For this purpose, a 15% (w/v) aqueous gelatin solution was prepared, followed by the addition of phosphate buffer (10 mM, pH 3.5; 20 mL). The mixture was sonicated for 30 minutes to facilitate gelatin degradation and then filtered through a 0.22 µm membrane filter. Resveratrol solutions at concentrations of 4 µg/mL, 12 µg/mL, and 18 µg/mL were prepared from the stock solution, injected in triplicate, and analyzed using the HPLC system.

Limit of Quantification and Detection

The limit of detection (LOD) and limit of quantification (LOQ) were estimated using the serial dilution approach in accordance with the guidelines provided by the International Council for Harmonisation (ICH).[25]

Synthesis and characterization of PLGA polymer

PLGA polymer was synthesized through ring opening polymerization (ROP) adopting the procedure as reported previously.[26,27] For the synthesis of PLGA polymer, the monomers *dl-lactide* and *glycolide* were first purified prior to polymerization. The purification was carried out through azeotropic distillation for 12 h to remove residual moisture and impurities. After distillation, the monomers were further dried using a rotary evaporator. The dried monomers were then subjected to polymerization in the presence of stannous 2-ethylhexanoate (0.1% w/v) as a catalyst under vacuum conditions for 8 h.

The resulting polymer was purified by dissolving it in dichloromethane (DCM) followed by precipitation in cold isopropyl alcohol (IPA). This purification step was repeated twice to ensure removal of unreacted monomers and impurities. The purified polymer was subsequently dried in a vacuum dryer at 22°C. The synthesized PLGA was characterized to determine its weight average molecular weight (Mw), number average molecular weight (Mn), polydispersity index (PDI), and the lactic acid to glycolic acid (LA/GA) ratio. These parameters were analyzed using gel permeation chromatography (GPC) and proton nuclear magnetic resonance (^{1}H NMR) spectroscopy, respectively.

GPC analysis was performed using HPLC-grade chloroform as the mobile phase. The solvent was filtered through a 0.22 µm membrane filter and sonicated for 60 min prior to use. Chromatographic analysis was carried out at 35°C using a Shimadzu LC-10AD HPLC pump coupled with a Shimadzu RID-6A refractive index detector. A Styragel HR4 column was employed in isocratic mode with a mobile phase flow rate of 1 mL/min. The injection volume for each sample was 100 µL, and the obtained chromatograms were processed using “GPC for Class-VP” software.

The ratio of lactic acid to glycolic acid in the synthesized PLGA was determined by ^{1}H NMR spectroscopy. For analysis, a small amount of the polymer was dissolved in deuterated chloroform ($CDCl_3$) and examined using a Bruker Avance DPX-300 NMR spectrometer. Tetramethylsilane (TMS) was used as the internal reference standard, and its

signal was assigned as zero chemical shift. The spectrum was recorded over a chemical shift range of 0-11 ppm, and the LA/GA ratio was calculated from the corresponding peak integrations.

Cytomodulin coupling and characterization of porous scaffold

Porous PLGA microparticles were fabricated using a water-in-oil-in-water (w/o/w) double emulsion solvent evaporation technique, with ammonium bicarbonate serving as a gas-forming porogen to generate a porous structure.[27]

Briefly, PLGA (200 mg) was dissolved in dichloromethane (DCM, 4 mL). Separately, an aqueous ammonium bicarbonate solution (15%, 1 mL) was prepared and introduced into the PLGA solution to form the primary emulsion.

The mixture was homogenized at 5000 rpm for 5 min to obtain a stable water-in-oil emulsion.

The resulting primary emulsion was then added dropwise into a beaker containing polyvinyl alcohol (PVA) solution (200 mL, 0.5% w/v) under continuous stirring to form the secondary emulsion. The organic solvent was allowed to evaporate, resulting in the formation of porous microparticles. The particles were collected, washed three times with distilled water to remove residual stabilizer and reagents, and subsequently lyophilized.

To introduce reactive functional groups on the particle surface, the microparticles were treated with 0.01 M sodium hydroxide (NaOH), which hydrolyzed the surface ester bonds and generated free carboxylic acid groups. Cytomodulin was then immobilized onto the porous microparticles through carbodiimide-mediated coupling using 1-ethyl-(3,3-dimethylaminopropyl) carbodiimide (EDC) and N-hydroxysuccinimide (NHS) in acetate buffer. Following the coupling reaction, the particles were washed three times with distilled water and freeze-dried to obtain free-flowing functionalized microparticles.

Preparation of Resveratrol-Loaded Gelatin Gel

A gelatin gel (15% w/v) was prepared by dissolving gelatin in distilled water maintained at approximately 50 °C to obtain a clear aqueous solution. A stock solution of resveratrol (25 mg/mL) was prepared using acetone as the organic solvent. Different concentrations of resveratrol (2.5, 5, and 10 mg/mL) were incorporated into the gelatin gel using a nanoprecipitation technique. In this method, resveratrol was first dissolved in acetone to form the organic phase. The resulting solution was then added dropwise into the aqueous gelatin solution (15% w/v) under continuous stirring, leading to the formation of resveratrol nanoparticles within the gelatin matrix. The proportion of acetone to gelatin solution was optimized by adjusting the volume of acetone added to the gelatin phase to achieve stable nanoparticle formation and uniform drug distribution.

Fabrication of composite skin graft

Cytomodulin coupled porous microparticles (1%w/v) were dispersed in resveratrol loaded gelatin solution. Then, glutaraldehyde (GTA, 20 µl/ml) as cross linking agent was added in this solution to achieve gelation.

Characterization of composite skin graft

Morphology

Morphology and homogeneity of grafts (gelatin alone, gelatin-drug and gelatin-drug-PMS) were examined by scanning electron microscopy (S-3400N, Hitachi, Japan). Lyophilized gels were placed on double-sided tape, sputter coated with

gold for 30 sec under vacuum and examined in the microscope. SEM images were analysed using image analysis software.

Determination of cytomodulin coupling efficiency

The coupling efficiency of cytomodulin immobilized onto porous PLGA microparticles was quantified using the NanoOrange protein assay. Initially, the protein quantitation diluent was diluted tenfold with distilled water. The NanoOrange working reagent was prepared by diluting reagent component A 500-fold in the prepared quantitation diluent according to the assay protocol. A calibration curve was constructed over a concentration range of 10–300 ng/mL using bovine serum albumin (BSA) as the standard. For this purpose, a 1 µg/mL stock solution was prepared by diluting the BSA standard solution (2 mg/mL, component B). All samples and standards were incubated at 90–97 °C for 10 min, protected from light, and subsequently allowed to cool to room temperature for at least 20 min.

Fluorescence measurements were then performed using a fluorometer with excitation at 485 nm and emission detection at approximately 590 nm. The fluorescence intensity of the reagent blank was subtracted from the corresponding sample readings. A standard calibration curve of fluorescence intensity versus protein concentration was generated and used to determine the protein content in the analyzed samples.

Antioxidant activity assay

Resveratrol produces its antioxidant activity by two mechanisms either by scavenging the free radicals or by inhibiting enzymes which are responsible for the production of free radicals e.g. xanthine oxidase, etc. DPPH scavenging activity assay was carried out to show the free radical scavenging activity of resveratrol. Objective of this study was to confirm whether resveratrol was able to retain its antioxidant property while undergoing formulation development.

DPPH (2,2-diphenyl-1-picrylhydrazyl)scavenging activity assay

Resveratrol has free radical scavenging activity. DPPH is a stable free radical and can be used to determine the free radical scavenging activity of the drug [25]. DPPH (200 µM) solution was prepared in ethanol and stock solution of resveratrol (50 µg/ml) was prepared in DMSO. Resveratrol solution was further diluted using DMSO to prepare standard curve (2-10 µg/ml). DPPH (125, 200µM) was added to different concentration of resveratrol (125µl). It was incubated for 30 min at room temperature. Then absorbance was measured at 517 nm by using UV spectrophotometer.

The % scavenging effect of free radicals by resveratrol was calculated by equation 1. The graph of scavenging effect verses concentration was plotted to determine the SC_{50} (scavenging concentration) value.

$$\text{Scavenging effect } (\%) = \frac{Ab_{517}\text{control} - Ab_{517}\text{sample}}{Ab_{517}\text{control}} \times 100 \quad \ldots\ldots\ldots\ldots\ldots (1)$$

Where, Ab_{517} is the UV absorption at 517 nm

Micro shrinkage temperature

Micro shrinkage temperature is the temperature at which sample starts to shrink.[28] Micro shrinkage temperature was helpful to assess the hydrothermal stability of resveratrol loaded gelatin graft. Hydrothermal stability of a compound is the ability of a material to resist changes in physical shape or size as its temperature and water content changes. Micro shrinkage temperature of gelatin graft was increased after addition of drug it indicated that drug stabilized the gelatin

structure. In this study a small amount of graft material was taken with water on a grooved microscopic slide and then this slide was put on heating stage of hot stage microscope. Heating rate was 2°C/min, then micro shrinkage temperature was determined by taking optical microscopic images of sample.[29]

Fluid uptake property

This property of composite graft indicates its ability to absorb the fluid which is secreted during burn wound injury.[30]

In this experiment, graft was immersed in phosphate buffer saline solution and incubated at 37°C temperature. Weighed amount of sample was poured in wells of 24 well plates then GTA was added. Discs were cut with help of cork borer (diameter 8 mm) and weight was determined. Discs were immersed in PBS (pH 7.4) and withdrawn at preset time intervals. Extra water was soaked then final weight was determined and % water uptake was calculated from the equation 2.

$$\text{Fluid uptake property (\%)} = \frac{W_t - W_0}{W_0} \times 100 \quad \ldots\ldots\ldots\ldots\ldots (2)$$

Where, W_t is the final weight and W_0 is initial weight

Gelation time

Gelation is the property of a gelatin solution to form a gel or to convert in a solid [31]. It is affected by time, concentration and temperature. Resveratrol at different concentrations (2.5 mg/ml, 5 mg/ml and 10 mg/ml) was dispersed in 1mL aqueous solution of gelatin (15 %) in glass vials and GTA was added (20 µl/ml). Aqueous solutions of gelatin at different concentrations (10%, 15 % and 20 %) were taken in glass vials followed by addition of GTA (20 µl/ml). GTA at different concentrations (10 µl/ml, 20 µl/ml and 50 µl/ml) was added in the formulations (resveratrol 10 mg/ml and gelatin 15 %). Vials were kept under magnetic stirring using a stir bar at 37°C and gelling time was noted as the time required for the stir bar to stop.

Mechanical strength

For testing of mechanical strength, samples discs from different drug concentrations were prepared (15 mm in diameter and 4 mm in height) and studied for mechanical strength using texture analyzer (TAXT2, Stable Microsystems, UK) under “measure force in compression” mode. Pre-test speed and post-test speeds were kept as 1 mm/min and 3 mm/min respectively. The samples were compressed under the force provided by a 5 kg-load cell by using a cylindrical probe at test speed of 0.1 mm/min until the sample was broken down. Then maximum force required to break complete graft was recorded and it was plotted at different concentrations for all groups.

Degradation studies

Graft was prepared as in the case of *in vitro* release (described in preceding section) and incubated with 5mL PBS (pH 7.4, 10% Tween 80), at 37°C (n=3). Degradation of gels was followed at preset time intervals by aspirating the medium followed by freeze-drying it for the calculation of remaining weight (%) with respect to time. The morphology of degraded samples was also studied using SEM.

In vitro drug release study

In vitro drug release of resveratrol from graft at three different concentrations (0.25%, 0.5% and 1%) was carried out in PBS (100 mM, pH 7.4). In this study, samples were prepared in vials and allowed to undergo gelation for 1 h. Release

media (5 ml) was added to the each samples and incubated in a reciprocal shaker bath at 37°C and 100 rpm. At specific time intervals, an aliquot of release media (2 ml) was withdrawn and replaced with an equivalent amount of fresh media. Drug content in the samples was analyzed by validated HPLC analytical method at 373 nm.

RESULTS

HPLC method development and revalidation for resveratrol

HPLC analytical method was developed for quantitative determination of resveratrol from *in vitro* drug release samples. The stock solution of resveratrol was prepared in phosphate buffer (10 mM; pH 3.5, 5% tween 80) in which the solubility was found to be 1.3 mg/ml. Validation parameters are shown in table 1. Accuracy and Precision values for HPLC analytical method were within the limit of ICH guidelines (Accuracy- 95%-105% and Precision- less than 2% RSD).

Validation parameters

Percentage recovery was calculated from the differences between the peak areas obtained for injections of known concentrations and the calculated concentration. Retention time of resveratrol was found to be 5.4 min shown in fig. 6. Recovery values within limits (~ 95-105%) were obtained for each of the concentrations indicating that the method was accurate.

Table 1: Validation parameters of HPLC method for resveratrol.

Parameters	Values
Analytical wavelength (nm)	373
Linearity (µg/ml)	2-20
Slope (± RSD)	67386.4 (± 4.4)
Intercept	597.89(±3.1)
Correlation coefficient (R^2)	0.998 ± 0.00045
LOD (µg/ml)	0.33
LOQ (µg/ml)	1

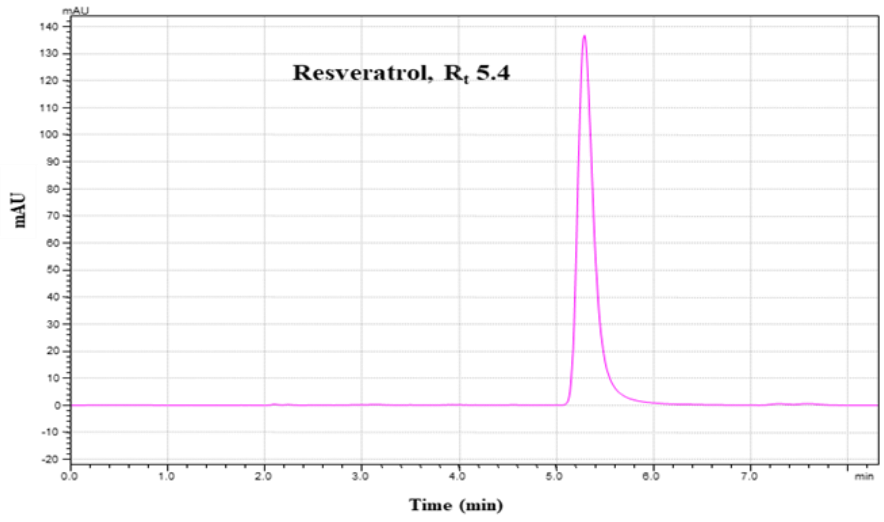

Fig. 1: Representative chromatogram of resveratrol.

Table 2: Inter-day and Intra-day accuracy and precision for resveratrol.

Conc. (µg/ml)	Intra-day		Inter-day	
	Accuracy	Precision	Accuracy	Precision
4	99.11	1.456	96.87	1.08
12	99.60	1.213	100.23	1.14
18	101.9	1.157	102.28	1.73

The developed method was found to be precise as the RSD value for precision study was less than 2%, and the method was found to be specific for the drug being analyzed in the presence of gelatin, as % recoveries of specificity samples were within the limits (95%-105%), as shown in table 2 and 3.

Table 3: Specificity of analytical method for resveratrol.

Actual concentration (µg/ml)	Calculated concentration (µg/ml)	% recovery
4	3.93	98.44
12	11.72	97.67
18	17.13	100.77

Synthesis and Characterization of PLGA polymer

The polymer was synthesized in bulk via ring-opening polymerization (ROP) with a batch size of 15 g, resulting in an overall yield of approximately 75%. The obtained polymer appeared translucent white in color. It was insoluble in water but readily dissolved in common organic solvents such as chloroform, acetone, and dichloromethane. The molecular characteristics of the synthesized polymer, including weight-average molecular weight (Mw), number-average molecular weight (Mn), and polydispersity index (PDI), were determined using gel permeation chromatography (GPC). The chromatographic analysis showed a retention time of approximately 7.8 min. The PDI value was calculated to be 1.7, indicating a relatively narrow molecular weight distribution with a symmetrical chromatographic peak. The Mn and Mw values obtained from GPC analysis were 73,622 Da and 125,521 Da, respectively. Proton nuclear magnetic resonance (^1H NMR) spectroscopy was employed to determine the lactic acid to glycolic acid (LA/GA) ratio in the synthesized polymer, which was found to be 2.7:7.3. For further experimental use, the polymer was stored at −20 °C after purging with nitrogen to prevent degradation.

Fabrication of composite skin graft

Fabrication and Characterization of porous scaffold and cytomodulin coupling

Porous PLGA microparticles were prepared by gas foaming w/o/w double emulsion method.[32] Then it was further hydrolyzed and coupled with cytomodulin using EDC and NHS as coupling agents. Average particle and pore size of microparticles was determined using SEM and found to be average 274 µm and 10.2 µm respectively. Cytomodulin was coupled on porous microparticles with an efficiency of 83.3% at 200 ng/ml initial concentration using BSA as standard.

Gelatin solution containing resveratrol

Resveratrol is a hydrophobic compound, which presents challenges for direct incorporation into hydrophilic gelatin solutions. To overcome this limitation, a nanoprecipitation technique was employed to facilitate the loading of resveratrol into the gelatin matrix. A resveratrol solution was first prepared in acetone (maximum solubility: 25 mg/mL) and then added dropwise into the gelatin solution under continuous stirring using a syringe. During this process, acetone diffuses into the aqueous gelatin phase, leading to the precipitation of resveratrol in the form of

nanoparticles within the gelatin matrix. However, due to the desolvating nature of acetone, excessive addition reduces the availability of water required to maintain gelatin in solution, resulting in the precipitation of hydrated gelatin chains. Therefore, the maximum allowable acetone-to-gelatin ratio was experimentally determined. It was observed that a ratio of 4:10 represented the upper limit, beyond which gelatin precipitation occurred. Based on this observation, three different acetone-to-gelatin ratios (1:10, 2:10, and 3:10) were investigated in the present study, corresponding to final resveratrol concentrations of 2.5 mg/mL, 5 mg/mL, and 10 mg/mL within the gelatin gel. These formulations were subsequently evaluated for key physicochemical and functional properties, including fluid uptake, gelation time, mechanical strength, and drug release behavior. The particle size of the resveratrol nanoparticles dispersed in the gelatin matrix was measured using a Zetasizer after appropriate dilution with purified water. The average particle size was found to be 602.5 nm with a polydispersity index (PDI) of 0.564. Based on the overall characterization results, the optimized resveratrol concentration was selected for further experimental studies.

Fabrication of composite skin graft

Cytomodulin coupled porous microparticles were dispersed in resveratrol loaded gelatin solution. Then, glutaraldehyde (GTA) as cross linking agent was added to this solution to achieve the required injectability of the graft and gelation was achieved. Cross-linking was mainly due to formation of Schiff's base between the ε-amino groups of lysine and hydroxylysine side groups of gelatin and the aldehyde groups of GTA.[33] It was further characterized and evaluated for *in vivo* and *in vitro* parameters.

Characterization of composite skin graft

Morphology

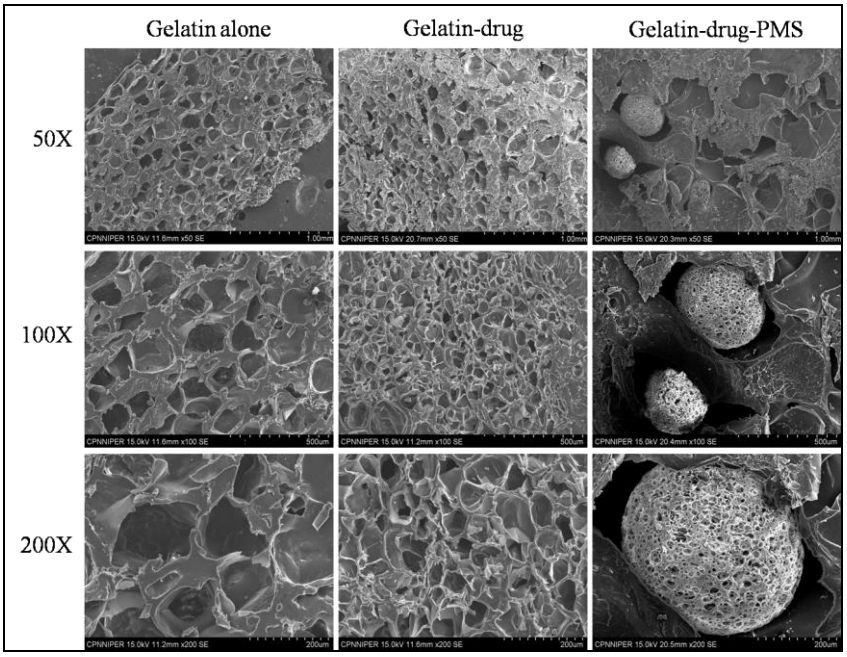

Fig. 2: Surface morphology of composite skin graft using scanning electron microscopy (SEM).

SEM showed visual images of interconnecting pores in gel-drug matrix and uniform distribution of drug and microparticles in gelatin matrix shown in fig. 2. Porous structure of microparticles demonstrated its suitability for facilitating cell migration, proliferation and cell growth. Particles size of microparticles was found to be average of 274 µm and pore size was found ~10.2 µm.

Cytomodulin coupling efficiency

Coupling efficiency of cytomodulin was determined using NanoOrange® reagent which enables accurate detection of proteins and peptides in solutions at concentration between 10 µg/ml-10 ng/ml. The reagent *per se* is virtually non fluorescent in aqueous solution, but upon interaction with proteins and peptides undergoes a significant fluorescence enhancement. A protein/peptide-bound form of NanoOrange® shows a broad excitation peak at 485 nm and a broad emission peak at 590 nm which directly depends on the concentration of protein/peptides a biomimetic peptide which mimic to TGF-β and helpful for skin cell regeneration and cell growth. It was coupled on porous PLGA microparticles with the help of EDC and NHS coupling agents. Coupling of cytomodulin (initial concentration was 200 ng/ml) on microparticles was found 83.3% using BSA as reference standard.

Antioxidant activity assay

DPPH is a stable, nitrogen-centered free radical which produces violet colour in ethanol solution. It was reduced to a yellow coloured product, diphenyl picryl hydrazine, with the addition of all fractions in a concentration-dependent manner. The DPPH radical had been used widely to investigate the scavenging activities of resveratrol.[34] DPPH radical was scavenged by antioxidants through the donation of hydrogen, forming the reduced DPPH-H•. The color changed from purple to yellow after reduction, which can be quantified by its decrease of absorbance at wavelength 517 nm. Radical scavenging activity of resveratrol in graft was tested by its ability to bleach the stable DPPH radical.

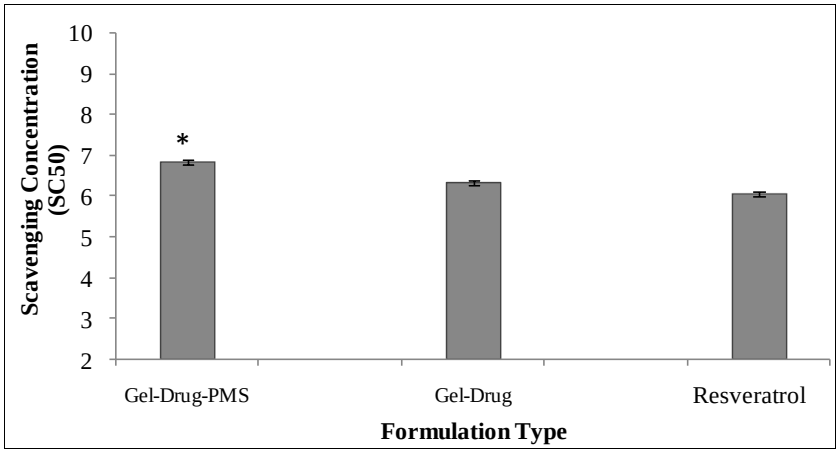

Fig. 3: SC_{50} (scavenging concentration) of formulations for antioxidant activity.

*p>0.05 vs gel-drug and pure resveratrol so no significant difference between formulations were observed

This method is based on the reduction of alcoholic DPPH solution in the presence of hydrogen donating anti-oxidant(AH) due to the formation of non- radical form DPPH–H by the reaction DPPH+AH→ DPPH–H +A. The remaining DPPH measured after certain time, corresponds inversely to the radical scavenging activity of the antioxidant. The sensitivity of the method is determined by the strong absorption of DPPH. This is rapid and simple analytical method which takes only 15 minutes and little man power, no expensive reagents or sophisticated instruments are required.[35] Antioxidant activity assay was carried out to show the ability of the resveratrol to scavenge free radicals after development of the composite graft. Lower the SC_{50} value of indicates better is the scavenging ability of the sample. SC_{50} value for resveratrol in gel-drug-PMS and gel-drug was calculated from standard graph, and found 6.8 µg/ml and 6.3 µg/ml respectively, which was close to pure resveratrol ($Sc_{50,}$ 6 µg/ml) from table 4.

Table 4: *In vitro* scavenging activity (%) of drug samples.

Concentration (µg/ml)	Absorbance	Scavenging activity (%)
DPPH alone	1.7013	0
1	1.1937	29.84
2.5	1.065	37.4
5	0.8904	47.66
7.5	0.7226	57.53
10	0.5957	64.99
Gel-Drug	0.784	53.92
Gel-Drug-PMS	0.83	51.50

Antioxidant activity was performed to measure the antioxidant potential of resveratrol after formulation development.

SC_{50} (scavenging concentration) is the concentration of antioxidant which reduces 50% of free radicals. As Gel-Drug and Gel-Drug-PMS both have SC_{50} value near to pure resveratrol, so it showed the same antioxidant activity as like pure resveratrol as shown in fig. 3. It indicated no loss in antioxidant activity of resveratrol after graft preparation.

Microshrinkage temperature

Shrinkage temperature is an important parameter used to evaluate the structural stability of graft materials. It refers to the temperature at which the graft begins to contract, commonly known as the microshrinkage temperature. In the present study, the formulation demonstrated stability in an aqueous environment at 37 °C, as the graft showed no evidence of shrinkage under these conditions (Table 5). Hot stage microscopy (HSM) images (Fig. 4) further confirmed that no noticeable shrinkage occurred up to approximately 55 °C for gelatin–drug–PMS as well as for crosslinked gelatin and gelatin–drug formulations. These observations indicate that the developed graft possesses adequate hydrothermal stability at physiological temperature and is therefore expected to remain stable at the intended application site.

Table 5: Changes in length of composite skin graft observed at 37°C and also that temperature was recorded at which changes were observed.

Sample	Initial length (µm)	Temperature (°C)		Length after shrinking (µm)	% Change in length
		No changes observed	Changes observed		
Gelatin alone	580	37	51	460	13.8
Gelatin-Drug	660	37	55	590	10.6
Gelatin-Drug-PMS	550	37	53	520	5.45

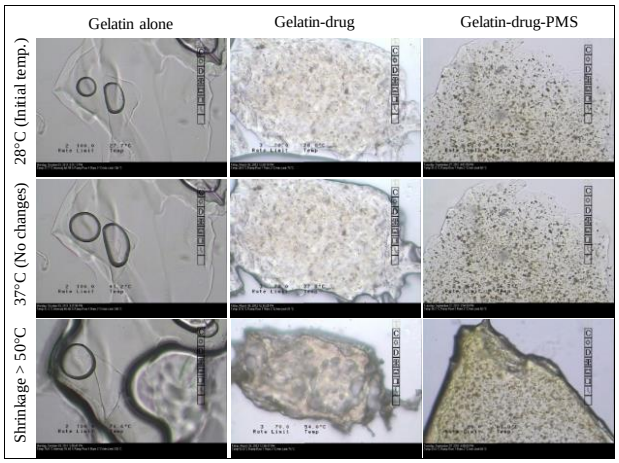

Fig. 4: Visual observation of changes in length of composite skin graft with different temperature.

Fluid uptake property

Fluid uptake capacity is a critical parameter for skin graft materials, as it directly influences the ability of the dressing to maintain a moist microenvironment at the burn wound site. An ideal synthetic graft should possess biocompatible and biomimetic characteristics that support fibroblast proliferation, collagen deposition, and extracellular matrix remodeling, thereby promoting effective tissue regeneration. At the same time, the graft should maintain an optimal moisture balance by absorbing excess wound exudate while preventing excessive dehydration of the wound bed during the healing process.[36]

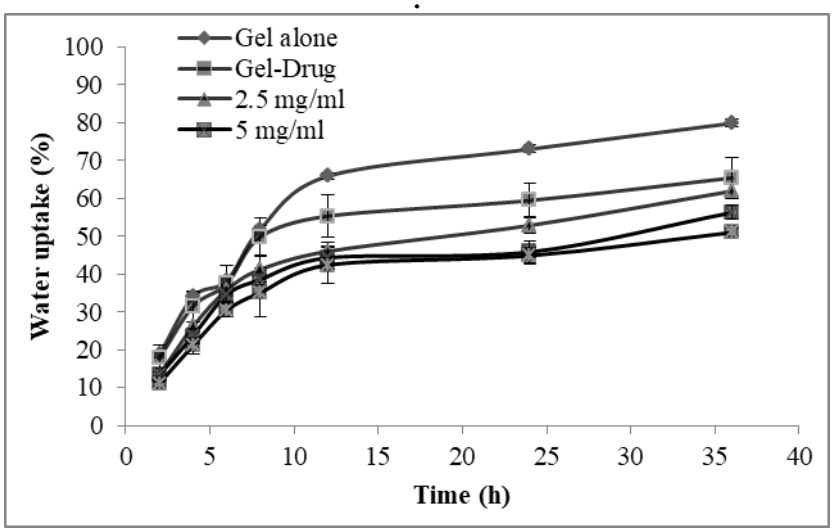

Fig. 5: Water uptake (%) of crosslinked gelatin, gelatin-drug and gelatin-drug-porous microparticles.

The fluid uptake study demonstrated that the developed graft exhibited a notable capacity to absorb burn wound exudates. This behavior can primarily be attributed to the hydrophilic nature of the gelatin matrix, which facilitates water absorption and swelling. Increased hydrophilic content within the graft structure enhances its fluid absorption capability, thereby enabling efficient management of wound exudates. However, the incorporation of resveratrol and PLGA microparticles slightly reduced the fluid uptake capacity of the composite formulation (GEL–Drug–PMS) compared with gelatin alone and gelatin–drug systems. This reduction may be attributed to the relatively hydrophobic nature of resveratrol and PLGA, which partially limits the availability of hydrophilic domains responsible for water absorption. Nevertheless, as resveratrol does not chemically interact with the gelatin matrix, variations in drug concentration did not significantly influence the overall fluid uptake behavior of the graft. The results further indicated that the composite graft was capable of absorbing approximately 50% of its own weight in fluid, suggesting its potential effectiveness in managing burn wound exudates. Importantly, formulations containing different drug concentrations did not exhibit statistically significant differences in fluid absorption capacity. Despite containing nearly 85% inherent water content, the graft was able to absorb an additional 50% fluid without compromising its structural integrity, as illustrated in Fig. 5. This observation highlights the mechanical stability and swelling resilience of the developed hydrogel system, indicating that it can effectively handle wound exudates while maintaining its physical structure throughout the healing period. Efficient fluid management is particularly important for burn wounds, as excessive accumulation of wound exudate may lead to maceration of surrounding tissues and increase the risk of bacterial contamination. Therefore, a graft material must possess an optimized fluid uptake capacity that enables absorption of exudates without causing excessive drying of the wound environment. Hydrogel-based grafts typically exhibit limited additional fluid uptake due to their already high intrinsic water content (approximately 70–90%).[37]

However, this characteristic also provides the advantage of preserving structural integrity even after absorbing wound fluid. Similar observations have been reported in previous studies. For example, Balakrishnan et al. developed an alginate dialdehyde–gelatin hydrogel dressing that exhibited approximately 5% additional fluid uptake in addition to its initial 85% water content while maintaining structural stability [38]. Overall, the present findings suggest that the developed composite graft possesses an appropriate balance between hydrophilicity and structural integrity, enabling efficient absorption of burn wound exudates while maintaining a moist and stable healing environment.

Gelation time

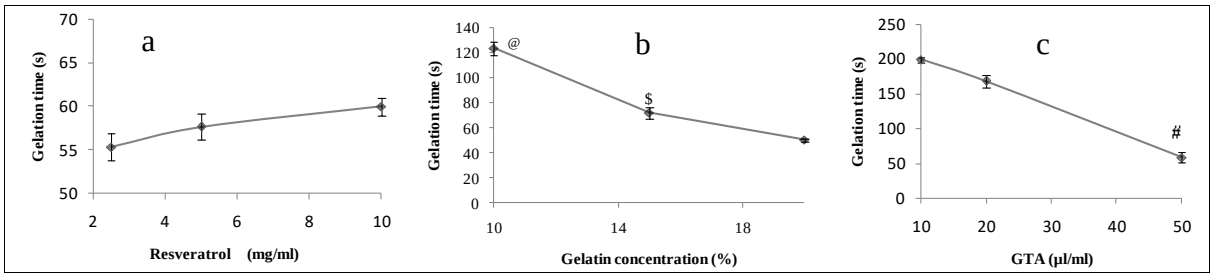

Fig. 6: Affect of (a) Resveratrol concentration, (b) Gelatin concentration and (c) GTA concentration on gelation time@ @p<0.05 vs 15% and 20%, $p<0.05 vs 20% gelatin concentration, #p<0.05 vs 10 µl and 20 µl and &p<0.05 vs 10 µl

GTA concentration

Gelation time is an important parameter governing the applicability of hydrogel-based graft systems, particularly for injectable or in situ forming biomaterials. In the present study, gelation time was found to decrease with increasing concentrations of glutaraldehyde (GTA), gelatin, and resveratrol-containing formulation components. The reduction in gelation time with increasing GTA concentration can be attributed to the enhanced availability of aldehyde functional groups, which readily react with the free ε-amino groups (–NH_2) of lysine and hydroxylysine residues present in gelatin. This reaction proceeds through a nucleophilic addition mechanism, leading to the formation of imine (Schiff base) linkages that facilitate rapid crosslinking within the gelatin network (Fig. 6c). Consequently, higher concentrations of GTA accelerate the formation of the crosslinked polymeric network, thereby reducing the gelation time. Similarly, an increase in gelatin concentration also contributed to faster gel formation (Fig. 6b). Higher gelatin content increases the availability of reactive amino groups that participate in crosslinking with GTA. In addition, elevated polymer concentration promotes stronger protein–protein and protein–solvent interactions, resulting in a denser molecular network. The greater number of intermolecular interactions and crosslinking sites enables the system to achieve structural stabilization more rapidly, thereby shortening the gelation time. In contrast, variations in resveratrol concentration did not significantly influence the gelation behavior of the system (Fig. 6a). This observation can be explained by the fact that resveratrol was incorporated into the gelatin matrix in nanoparticulate form rather than as a molecularly dissolved species. As a result, the drug remains physically dispersed within the matrix without participating in chemical interactions with the gelatin chains. Since resveratrol lacks reactive functional groups capable of forming covalent bonds with the gelatin network under the experimental conditions, its presence does not interfere with the crosslinking process or alter the gelation kinetics. Therefore, the gelation time remained largely unaffected by changes in drug concentration. Overall, these findings indicate that gelation behavior of the developed graft is primarily governed by the crosslinking density and polymer concentration, while the incorporation of resveratrol nanoparticles does not compromise the gelation characteristics of the gelatin-based hydrogel system.

Mechanical strength

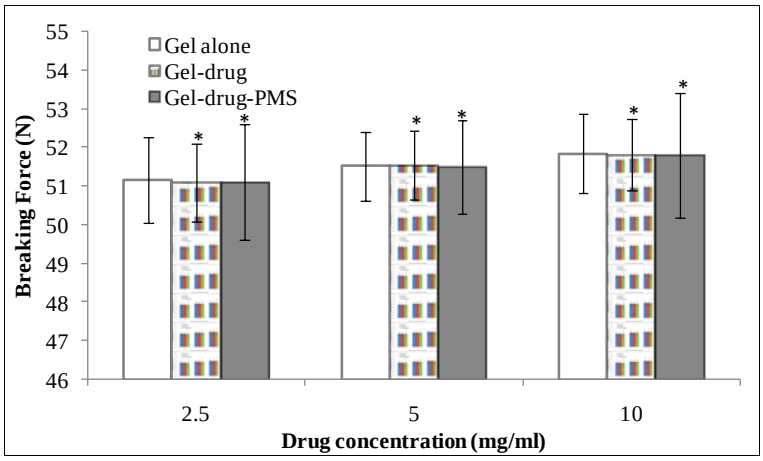

Fig. 7: Breaking force of composite skin graft containing different resveratrol concentrations in comparison to drug containing gel and gel alone. *P>0.05 vs other grafts.

Mechanical strength of different grafts was measured using texture analyzer as maximum force required to breaking of graft after 1 hr post gelation with GTA. No significant difference was found between different groups in comparison to gelatin alone. As resveratrol is present in particulate form in formulation so no interaction occurs between drug and other components. There is no significant changes were observed as increasing drug concentration and different types of grafts shown in fig. 7.

Breaking force is also the indicator of graft to resist fragmentation allow provide sufficient strength during healing period. Since graft have ~50N breaking force that good enough to resist degradation and fragmentation.

***In vitro* degradation**

The degradability of the hydrogels was studied by examining the weight loss of gels with time in PBS at 37°C. A linear decrease in weight with time was seen up to 4 weeks with complete dissolution of the gel at the end of 5 weeks demonstrating the degradability of the matrix was visually observed by SEM images shown in fig. 8. Biodegradability of the skin graft is important to provide an adequate space for neotissue formation.

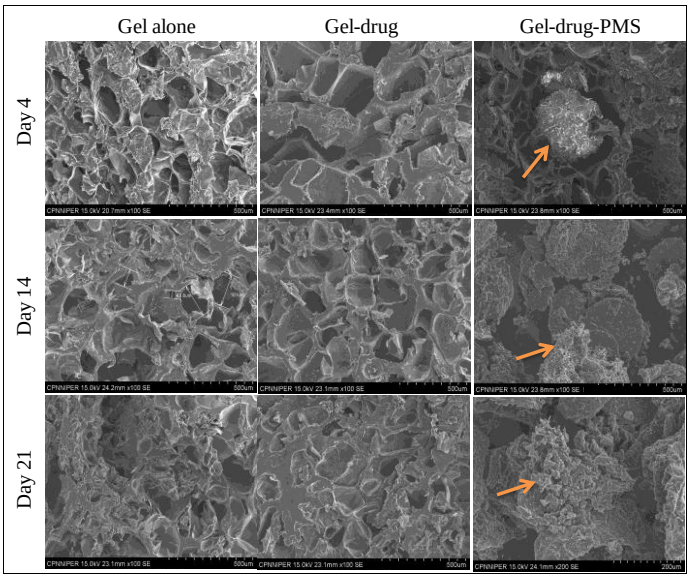

Fig. 8: Visual observation of *In vitro* degradation profile of composite skin graft.

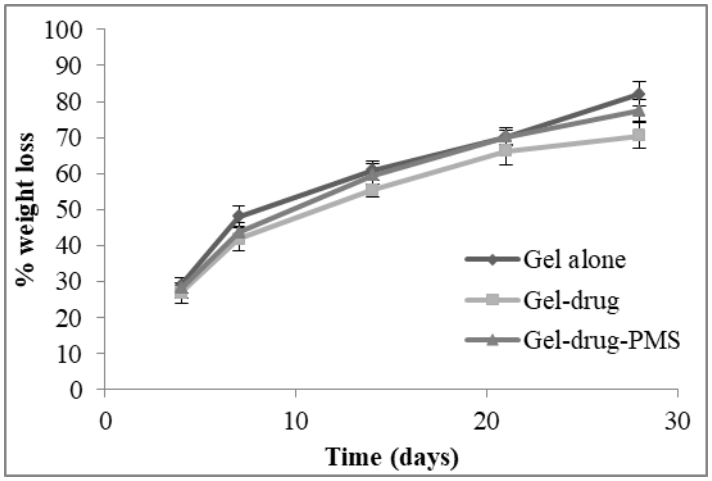

Fig. 9: *In vitro* degradation profile of composite skin graft (n=3).

*p<0.05 vs gel alone and gel-drug-PMS,@p<0.05 vs gel alone

Considering the tendency of skin grafts to adhere to the wound bed, their biodegradability becomes even more important to circumvent the need of removal of the skin graft after healing has occurred, which might otherwise disturb the tissue undergoing healing process. In this study, composite graft consisted of components which are biodegradable in nature and their biodegradability was evaluated shown in fig. 9. Degradation showed that gel alone has higher biodegradation followed gel-drug-PMS then gel-drug.

Evaluation of composite skin graft

In vitro drug release

Resveratrol at different drug concentrations (2.5 mg/ml, 5 mg/ml and 10 mg/ml) was dispersed in gelatin and further cross linked by glutaraldehyde. Cumulative release (%) was found to be 87%, 85% and 75% to the concentrations of 10 mg/ml, 5 mg/ml and 2.5 mg/ml respectively for 5 days. Mass balance studies shown the remaining amount of drug in concentrations of 10 mg/ml, 5 mg/ml and 2.5 mg/ml is 11.8%, 13.2% and 21.1% respectively.

For inhibiting free radicals in the burn area, it is desirable drug concentration should be present at the wound site during initial time point to inhibit further tissue damage by free radicals, which are generate during the initial trauma, followed by a prolonged sustained drug release at a therapeutically effective level to inhibit latent damage during the course of burn healing. The developed composite graft of 10 mg/ml resveratrol concentration exhibited 87% sustain release of drug during the initial 5 days shown in fig. 10.

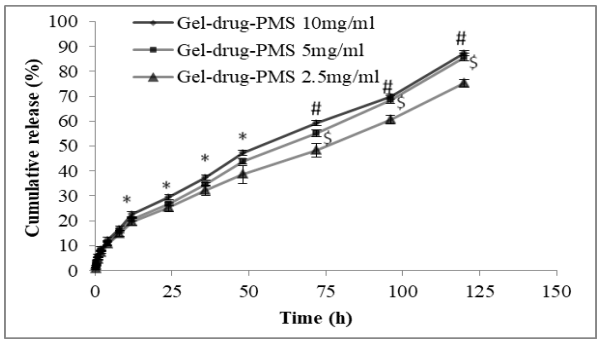

Fig.10: *In vitro* drug release profile of resveratrol from composite skin graft (n=3).

*p<0.05 vs loading 2.5 mg/ml, #p<0.05 vs loading 2.5 and 5 mg/ml and $p<0.05 vs 2.5 mg/ml.

DISCUSSION

The experimental findings collectively demonstrate the successful development and characterization of a resveratrol-loaded, injectable composite graft system. The HPLC analytical method developed for quantifying resveratrol in in vitro release samples proved to be reliable and reproducible. The method showed excellent accuracy (95–105%) and precision (RSD < 2%), in accordance with ICH guidelines. The distinct retention time of 5.4 min confirmed good specificity, with no interference from gelatin, ensuring dependable drug estimation throughout the study.

The synthesized polymer, prepared via ring opening polymerization with a 75% yield, exhibited desirable physicochemical characteristics. GPC analysis revealed a relatively narrow molecular weight distribution (PDI 1.7), indicating uniform polymer chains. The molecular weight values (Mn: 73,622 Da; Mw: 125,521 Da) and LA/GA ratio (2.7/7.3) confirmed successful synthesis. The polymer's solubility in organic solvents and stability under nitrogen at −20°C further supported its suitability for scaffold fabrication.

Porous PLGA microparticles prepared by the gas foaming double emulsion method showed uniform morphology with an average particle size of 274 µm and pore size of 10.2 µm. Efficient coupling of cytomodulin (83.3%) demonstrated successful surface functionalization, enhancing the bioactive potential of the system.

Since resveratrol is hydrophobic, nanoprecipitation was effectively employed to enable its incorporation into hydrophilic gelatin. Optimization of the acetone-to-gelatin ratio prevented gelatin precipitation, with 4:10 identified as the maximum tolerable ratio. The resulting nanoparticles (≈602 nm) were successfully embedded within the gelatin matrix. Finally, cross-linking with glutaraldehyde provided appropriate injectability and gelation through Schiff's base formation, yielding a stable and functional composite graft suitable for further biological evaluation.

The in vitro characterization confirmed the structural integrity and functional performance of the developed composite graft. SEM images clearly revealed an interconnected porous network within the gel–drug matrix, along with uniform distribution of both resveratrol and microparticles throughout the gelatin scaffold. The average microparticle size (274 µm) and pore size (~10.2 µm) were appropriate for promoting cell migration, proliferation, and tissue integration, indicating suitability for regenerative applications.

Cytomodulin, a biomimetic peptide mimicking TGF-β activity, was successfully conjugated onto porous PLGA microparticles using EDC–NHS chemistry. The NanoOrange® assay demonstrated a high coupling efficiency of 83.3%, confirming effective surface functionalization. This suggests that the system can provide sustained biological cues to support skin cell regeneration.

The antioxidant potential of resveratrol after formulation was assessed using the DPPH assay. Both Gel-Drug and Gel-Drug-PMS formulations exhibited SC50 values (6.3 and 6.8 µg/ml, respectively) close to that of pure resveratrol, indicating that the formulation process did not compromise its free radical scavenging ability. This confirms the preservation of resveratrol's therapeutic activity within the graft matrix.

Thermal stability studies further supported formulation robustness. No shrinkage was observed up to ~55°C, and the graft remained stable at physiological temperature (37°C), demonstrating good hydrothermal stability. Additionally, appropriate fluid uptake capacity suggests the graft can maintain a moist wound environment-an essential factor for

effective burn healing and tissue regeneration. Overall, the results highlight the structural, biochemical, and functional suitability of the developed graft for skin repair applications.

The fluid uptake study demonstrated that the developed graft possesses an optimal ability to manage burn wound exudates. Owing to the hydrophilic nature of gelatin, the graft was able to absorb nearly 50% of its own weight in fluid, even though it already contained approximately 85% water. This indicates that the formulation can effectively handle excess wound secretion without losing structural integrity. Although the inclusion of hydrophobic resveratrol and PLGA microparticles slightly reduced the fluid uptake in the composite graft (Gel-Drug-PMS) compared to gel alone, the absorption capacity remained sufficient for burn management. Importantly, varying drug concentrations did not significantly influence fluid uptake, confirming that resveratrol does not interact with gelatin in a way that alters this property.

Maintaining a balanced fluid absorption is critical in burn care—excess exudate can lead to maceration and infection, whereas excessive absorption may cause dehydration. The results suggest that the graft achieves this balance effectively, similar to previously reported hydrogel systems, while maintaining mechanical stability.

Gelation studies showed that increasing concentrations of glutaraldehyde (GTA) and gelatin reduced gelation time due to enhanced Schiff base formation between aldehyde and amino groups. In contrast, changes in resveratrol concentration did not affect gelation, as the drug exists in nanoparticulate form and does not chemically interact with gelatin. Mechanical strength analysis further confirmed that the incorporation of drug and microparticles did not compromise graft integrity. Overall, the findings indicate that the composite graft is structurally stable, functionally balanced, and well-suited for burn wound healing applications.

The results indicate that resveratrol, being present in nanoparticulate form, did not chemically interact with gelatin or other graft components. Consequently, increasing drug concentration or modifying graft composition did not significantly affect mechanical performance. All graft variants exhibited a breaking force of approximately 50 N, which is sufficient to resist fragmentation and provide the mechanical stability required during the healing period.

Degradation studies in PBS at 37°C showed a steady, linear weight loss over four weeks, with complete dissolution by the fifth week. SEM observations further confirmed gradual matrix breakdown. Such controlled biodegradability is highly desirable, as it creates space for new tissue formation while eliminating the need for graft removal after healing—thereby minimizing additional trauma to regenerating tissue. Among the formulations, gel alone degraded fastest, followed by Gel-Drug-PMS and Gel-Drug, indicating that drug and microparticle incorporation slightly modulated degradation behavior.

Drug release studies demonstrated sustained resveratrol release over five days, with cumulative release of 87%, 85%, and 75% for 10, 5, and 2.5 mg/ml concentrations, respectively. Mass balance analysis confirmed minimal residual drug in the matrix. Notably, the 10 mg/ml formulation provided a desirable release profile—ensuring higher drug availability during the critical early phase of burn injury to combat oxidative stress, followed by continued release to prevent delayed tissue damage. Overall, the composite graft combines adequate strength, controlled biodegradability, and sustained antioxidant delivery, making it promising for burn wound healing applications. Further the promising *in*

vitro results should be supported by *in vivo* studies which is in progress after due approval of Institutional Animal Ethics Committee (IAEC).

DECLARATIONS

ETHICS APPROVAL AND CONSENT TO PARTICIPATE

Not applicable

HUMAN AND ANIMAL RIGHTS

Research Involving Animals

Not applicable

CONSENT FOR PUBLICATION

All the authors read and approve the final version of manuscript for publication.

AVAILABILITY OF DATA AND MATERIALS

Data will be made available when required.

FUNDING

All the expenses for the experiments, and human resources involved were provided by Narayan Institute of Pharmacy, Gopal Narayan Singh University, Jamuhar, Sasaram, Bihar- 821305.

Conflict of Interest

All the authors declare no conflict of interest either financial or personal.

ACKNOWLEDGEMENTS

The authors sincerely acknowledge Gopal Narayan Singh University for providing access to journal articles.

Author Contributions

RR conceptualizes the research and methodology of the experiments, DK written original draft of the manuscript. VK performed formal analysis and investigations.

REFERENCES

1. Żwierełło W, Piorun K, Skórka-Majewicz M, Maruszewska A, Antoniewski J, Gutowska I. Burns: classification, pathophysiology, and treatment: a review. International journal of molecular sciences, 2023; 24(4): 3749.
2. Mahajan N, Soker S, Murphy SV. Regenerative medicine approaches for skin wound healing: from allografts to engineered skin substitutes. Current Transplantation Reports, 2024; 11(4): 207-21.
3. Yakupu A, Zhang J, Dong W, Song F, Dong J, Lu S. The epidemiological characteristic and trends of burns globally. BMC public health, 2022; 22(1): 1596.
4. van Niekerk A. Burn-related injuries. Oxford Research Encyclopedia of Global Public Health, 2022.
5. Gerstl JV, Ehsan AN, Lassarén P, Yearley A, Raykar NP, Anderson GA, et al. The global macroeconomic burden of burn injuries. Plastic and reconstructive surgery, 2024; 153(3): 743-52.

6. Radzikowska-Büchner E, Łopuszyńska I, Flieger W, Tobiasz M, Maciejewski R, Flieger J. An overview of recent developments in the management of burn injuries. International journal of molecular sciences, 2023; 24(22): 16357.
7. Palmieri TL. Emerging therapies for full-thickness skin regeneration. Journal of Burn Care & Research. 2023;44(Supplement_1):S65-S7.
8. Betz RR. Limitations of autograft and allograft: new synthetic solutions. Orthopedics, 2002; 25(5): S561-S70.
9. Katiyar S, Singh D, Kumari S, Srivastava P, Mishra A. Novel strategies for designing regenerative skin products for accelerated wound healing. 3 Biotech, 2022; 12(11): 316.
10. Sheridan RL, Tompkins RG. Skin substitutes in burns. Burns, 1999; 25(2): 97-103.
11. Vaporidou N, Peroni F, Restelli A, Jalil MN, Dye JF. Artificial Skin Therapies; Strategy for Product Development. Advances in Wound Care, 2023; 12(10): 574-600.
12. Socci MC, Rodríguez G, Oliva E, Fushimi S, Takabatake K, Nagatsuka H, et al. Polymeric materials, advances and applications in tissue engineering: a review. Bioengineering, 2023; 10(2): 218.
13. Sierra Sánchez Á. Design, development, analysis and comparison of human tissue-engineered skin substitute models. Universidad de Granada, 2024.
14. Maskan Bermudez N, Sa BC, Hargis A, Yaghi M, Mervis J. Skin grafting for dermatologists: past, present, and future. Current Dermatology Reports, 2024; 13(2): 47-54.
15. Pan J-f, Liu N-h, Sun H, Xu F. Preparation and characterization of electrospun PLCL/poloxamer nanofibers and dextran/gelatin hydrogels for skin tissue engineering. PLoS One, 2014; 9(11): e112885.
16. Kaur G, Narayanan G, Garg D, Sachdev A, Matai I. Biomaterials-based regenerative strategies for skin tissue wound healing. ACS Applied Bio Materials, 2022; 5(5): 2069-106.
17. Zhu J, Li Z, Zou Y, Lu G, Ronca A, D'Amora U, et al. Advanced application of collagen-based biomaterials in tissue repair and restoration. Journal of Leather Science and Engineering, 2022; 4(1): 30.
18. Sanz-Horta R, Matesanz A, Gallardo A, Reinecke H, Jorcano JL, Acedo P, et al. Technological advances in fibrin for tissue engineering. Journal of tissue engineering, 2023; 14: 20417314231190288.
19. Guo R, Xu S, Ma L, Huang A, Gao C. The healing of full-thickness burns treated by using plasmid DNA encoding VEGF-165 activated collagen–chitosan dermal equivalents. Biomaterials, 2011; 32(4): 1019-31.
20. Kelangi SS, Theocharidis G, Veves A, Austen WG, Sheridan R, Goverman J, et al. On skin substitutes for wound healing: Current products, limitations, and future perspectives. Technology, 2020; 8(01n02): 8-14.
21. Snyder D, Sullivan N, Margolis D, Schoelles K. Skin substitutes for treating chronic wounds, 2020.
22. Hill DM, Hickerson WL, Carter JE. A risk-benefit review of currently used dermal substitutes for burn wounds. Journal of Burn Care & Research, 2023; 44(Supplement_1): S26-S32.
23. Jiang X, Zhu Y, Chen P, Liu D. Biomimetic nanofibers with cell membrane functionalization for enhanced tissue engineering. Biomaterials Science, 2025; 13(12): 3176-91.
24. Mittal A, Chitkara D, Kumar N. HPLC method for the determination of carboplatin and paclitaxel with cremophorEL in an amphiphilic polymer matrix. Journal of chromatography B., 2007; 855(2): 211-9.
25. Kalita P, Medhi S, Borah S, Bhargav G, Alam F. Evaluation of Anti Inflammatory and Anti Oxidant Activities of Osbeckia crinite. Journal of Pharmaceutical Research International, 2022; 34(8B): 38-46.
26. Mishra N, Pandey V. Block Co-polymeric Nanocarriers: Design, Concept, and Therapeutic Applications. Springer, 2023.

27. Bulbake U, Jain S, Kumar N, Mittal A. Curcumin loaded biomimetic composite graft for faster regeneration of skin in diabetic wounds. Journal of Drug Delivery Science and Technology, 2018; 47: 12-21.
28. Shang M, Qiao H, He Z, Zhang Y, Liu X, Zhang Y, et al. Study on the shrinkage mechanism and prediction model of high-strength specified density concrete based on the internal curing micro-pump effect of MSW incineration tailings. Construction and Building Materials, 2023; 372: 130804.
29. Tao Y, Gu X, Wu H, Ni J, Hu Y, Wu D, et al. Ultralow Shrinkage 3D Transparent Nanoporous Glass Printing through Low-Temperature Sintering for Micro-Optical Applications. ACS nano, 2025; 19(35): 31643-55.
30. Gong X, Wang F, Yang J, Du H, Jiang M, Tan M, et al. Engineered composite dressing with exudate management capabilities for the process of entire wound healing. Materials Today Communications, 2024; 39: 108557.
31. Torrejon VM, Song J, Yu Z, Hang S. Gelatin-based cellular solids: Fabrication, structure and properties. Journal of Cellular Plastics, 2022; 58(5): 797-858.
32. Wu J, Ding J, Xiao B, Chen D, Huang D, Ma P, et al. A facile strategy for controlling porous PLGA microspheres via o/w emulsion method. Journal of Polymer Research, 2022; 29(12): 508.
33. Yu Z, Wu J, Zhang T, Chen C, Ma Y, Liu H, et al. Improving the crosslinking of collagen casing and glutaraldehyde by facilitating the formation of conjugate structure via pH. Collagen and Leather, 2024; 6(1): 29.
34. Hebbar K, Kumar N, Nataraj K, Basavaraj G, Prithviraj H, Suresha N, et al. Analysis of phytochemicals and evaluation of phenolic contents and antioxidant activities of Cissus javana. Journal of Advanced Scientific Research, 2024; 15(04): 32-8.
35. Vaidyaratnam PS, Sala AV. Indian medicinal plants , a compendium of 500 species, 2009; 1: 1481-5.